Chemical Methodologies 6(2022) 347-356

Chemical Methodologies

Journal homepage: http://chemmethod.com

Original Research Article

Synthesis and Characterization of New Inorganic Complexes and Evaluation Their Corrosion Inhibiter

Zahraa A. Rida*, Sahar S. Hassan, Sana H. Awad

Department of Chemistry, College of Science for Woman, University of Baghdad, Baghdad, Iraq

ARTICLE INFO

Article history

Submitted: 2022-01-24
Revised: 2022-03-08
Accepted: 2022-03-11
Manuscript ID: CHEMM-2201-1431
Checked for Plagiarism: **Yes**
Language Editor:
Ermia Aghaie
Dr. Behrouz Jamalvandi
Editor who approved publication:
Professor Dr. lotfali saghatforoush
DOI:10.22034/CHEMM.2022.326331.1431

KEYWORDS

Gelatin
Succinic anhydride
Carbon steel
Metal complexes
Corrosio

ABSTRACT

In this work, natural polymer Gelatin grafting was carried out with succinic anhydride by ring-opening polymerization then complexion with (Cr^{+3}), (Mn^{+2}), (Ni^{+2}), and (Zn^{+2}) was synthesized. The structure was characterized using FT-IR and UV-Vis. The results revealed that the structures of these complexes are Octahedral. The spectroscopic result of the ligand showed a bidentate behavior through the coordination via oxygen and nitrogen atoms. The newly synthesized polymers were tested as corrosion inhibitors on carbon steel alloy. The results of corrosion test indicated the corrosion decrease by using the new polymers on the service of the alloy. Inorganic polymers are appealing metals and alloys as corrosion inhibitors in various applications as they are cost-effective, renewable materials that are readily accessible, non-hazardous, possibly biodegradable, and biocompatible with the natural environment.

GRAPHICAL ABSTRACT

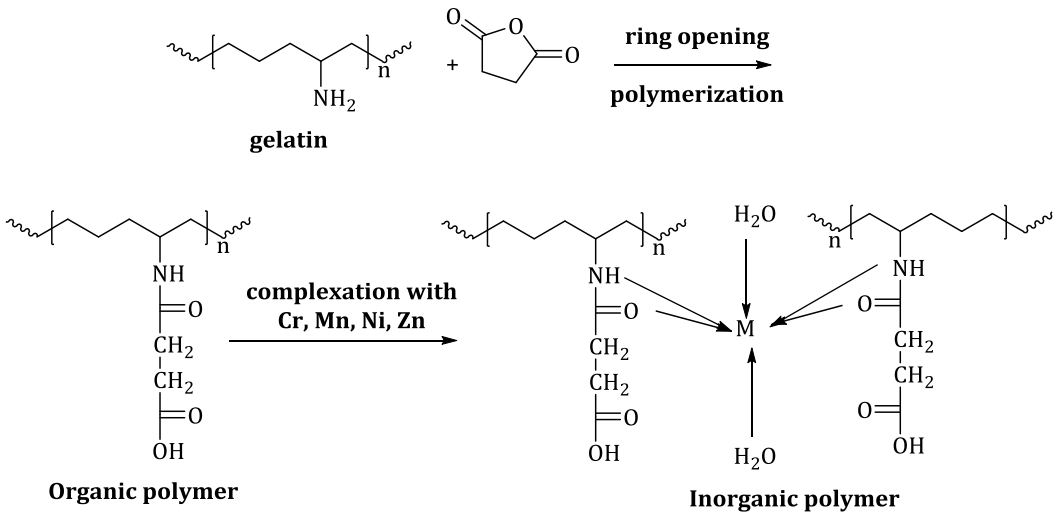

* Corresponding author: Zahraa A. Rida
✉ E-mail: zahraa.abd1205a@gmail.com

Introduction

The protein gelatin is made by boiling skin, tendons, ligaments, and bones in water. Cows and pigs are the most common sources. Gelatin is used in shampoos, face masks and other cosmetics as a thickening for fruit gelatins and puddings (such as Jell-O). It exists in sweets, marshmallows, cakes, ice cream, and yogurts, on photographic film and in vitamins as a coating and as capsules, as well as in "clearing" wines. Gelatin is not suitable for vegans. However, a vegan product is known as “agar" often sold as Gelatin. It is made out of a sort of seaweed [1]. When Gelatin is submerged in a liquid, it absorbs moisture and expands. The inflated particles melt as the liquid is warmed, generating a sol (fluid colloidal system) with the liquid, rising in viscosity and solidifying to create a gel when it cools. At higher temperatures, the gel state can be transformed to a sol state, and the sol can be turned back to a gel by cooling. Protein and sugar content, as well as temperature, influence setting time and tenderness [2]. The majority of Gelatin produced is used in the food business. The pharmaceutical business and other industries utilize Gelatin to make capsules, cosmetics, ointments, lozenges, and plasma products [3]. Photography as a business for print materials, a gelatin emulsion with barium sulfate, is applied first to give a smooth white surface. The emulsion of silver halide emulsions is made by mixing silver nitrate with an alkali halide solution in Gelatin; potassium bromide and iodide are commonly used. The silver halide that is then formed crystallizes into fine particles. The emulsion is made of remolded and is given a boost after chilling to a jelly, shredding, washing, speed, and contrast [4]. Succinic anhydride has the molecular formula $(CH_2CO)_2O$. It is an organic chemical. This white solid is succinic acid anhydride [5]. This substance may be made in the laboratory by dehydrating succinic acid. Succinic anhydride is produced industrially *via* catalytic hydrogenation of maleic anhydride with acetyl: Chloride or phosphoryl chloride or by thermal dehydration [6]. Succinic anhydride hydrolyzes readily to give succinic acid:

$$(CH_2CO)_2O + H_2O \rightarrow (CH_2CO_2H)_2$$

A similar reaction occurs with alcohols (ROH), resulting in the monoester

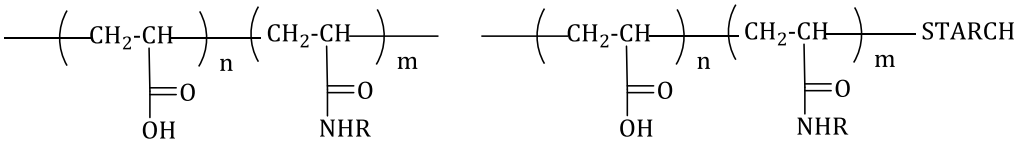

Random copolymer
crosslinked copolymer

Graft copolymer

Figure 1: Cross-linked copolymer

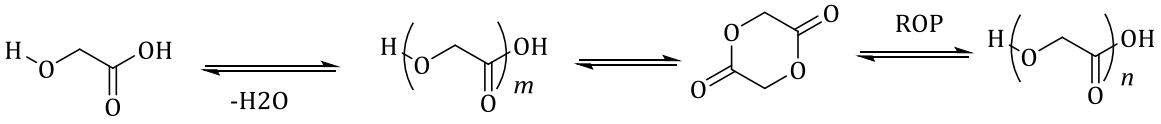

Oligomer Glicolide PGA

Figure 2: Ring-opening polymerization

An essential biological reaction is forming an amide bond between Gelatin with succinic anhydride. Natural polymers are among the most promising biomedical polymers [7]. Gelatin is a polyampholyte, biocompatible, biodegradable, edible, and soluble at body temperature. Polyelectrolyte complex coacervation of Gelatin with other bio polyelectrolytes and with modified natural polyelectrolytes is systematically summarized and described [8]. Recent and unique uses have focused on microencapsulation and drug delivery [9].

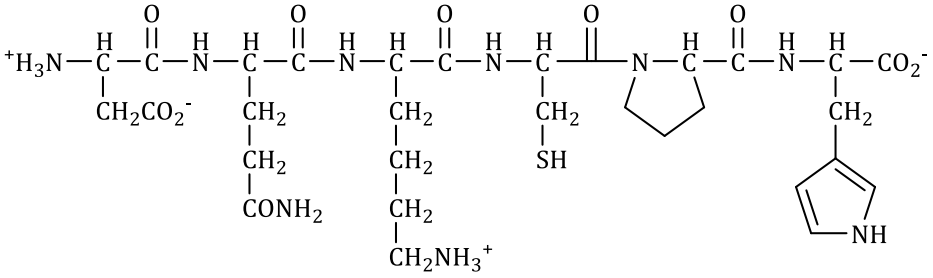

Figure 3: Chemical structure of Gelatin

Due to the inclusion of cell attaching and matrix metalloproteinase sensitive peptide motifs, Gelatin grafted methacrylate anhydride hydrogels mirror certain features of the extracellular template, allowing cells to flourish and spread in Gel MA-based scaffolds [10].

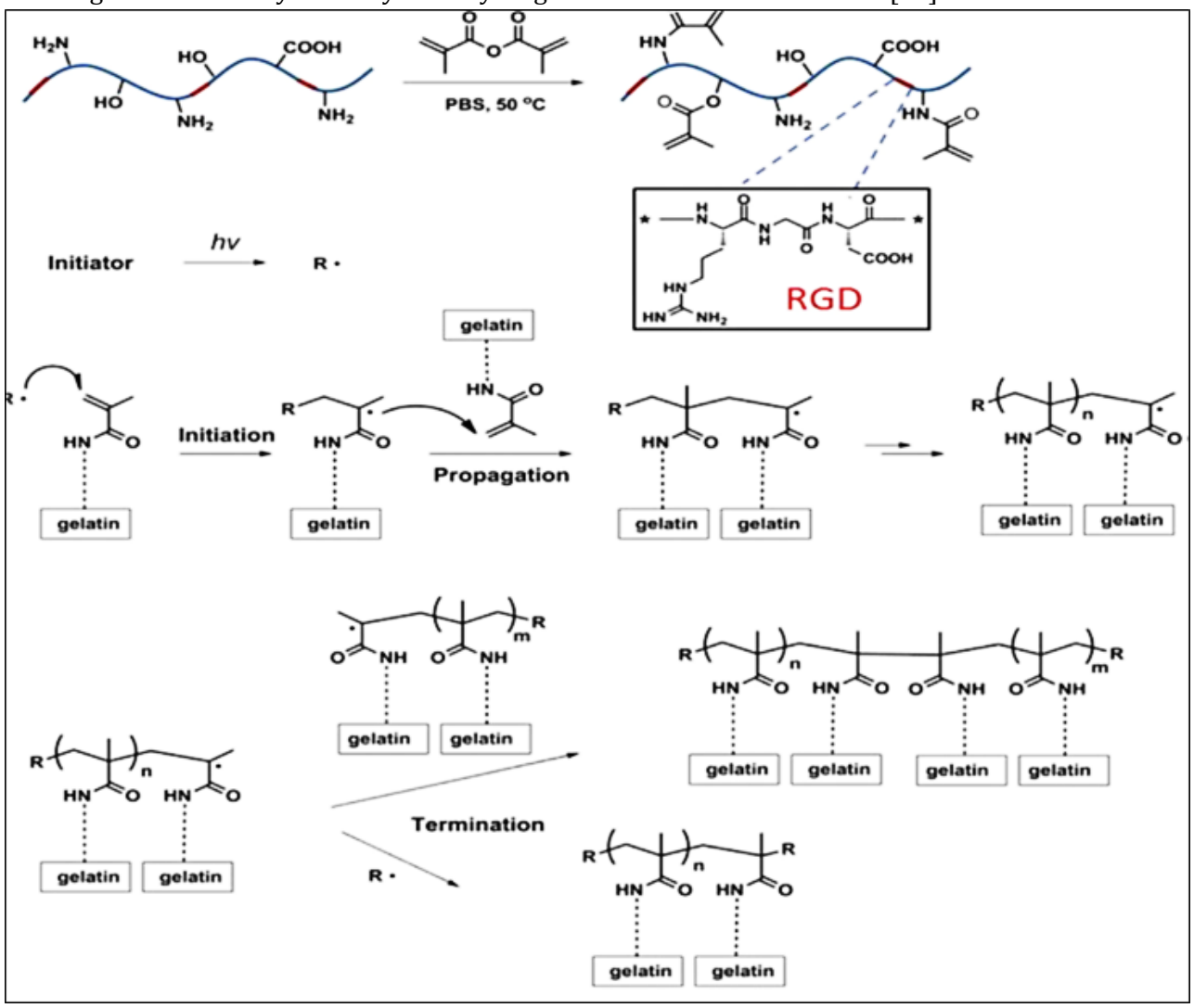

Figure 4: Gelatin grafting Mehta acrylate anhydride

The temperature utilized in the method changed the composition of the graft copolymer. Cross-linked gelatin biomaterials have found use in various ocular tissues, including attaching and supporting retinal tissue as a bio-adhesive [11] as a cellularized scaffold for the refurbishment and resuscitation of the corneal stoma, and as a cell-sheet carrier for corneal endothelial cells [12].

Metal corrosion is a major academic and industrial topic that has gotten much attention [13]. The removal of rust and scale in several industrial processes using the acid solution is common [14,15]. Forming a protective barrier over the carbon steel surface and removing water molecules is due to the blocking of the active sites,

decreasing the corrosion rate. This compound interacts with the anodic and, or catholic reaction [16,17]. This work accordingly aimed at studying the inhibitive (Complexes Cr^{+3}, Zn^{+2}) towards the corrosion of carbon steel in 0.5M hydrochloric acid at 25 °C temperatures and different concentrations of (complexes Cr^{+3}, Zn^{+2}) and studying potentiodynamic polarization measurements, weight loss, and open circuit potential.

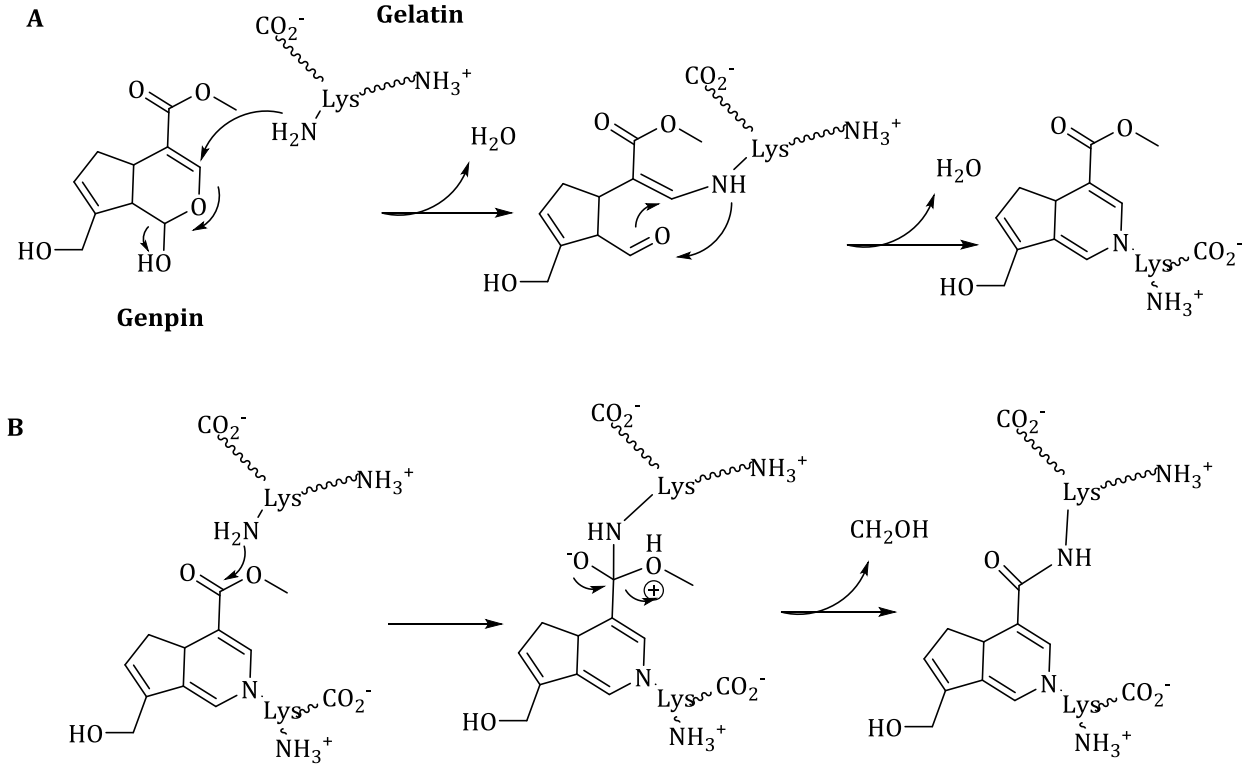

Figure 5: Gelatin that has been cross-linked

Material and Method

Gelatin was prepared from Himedia and was used as received. Succinic anhydride was obtained from Sigma-Aldrich. [$CrCl_3.6H_2O$], [$MnCl_3.4H_2O$], [$Ni(NO_3)_2.6H_2O$], [$ZnCl_2$]. They were obtained from Merck, DMF from Himedia, diethyl ether from Himedia, APS from Himedia.

Techniques

Melting points were determined in open capillary tubes, and FT-IR was recorded using [KBr] for ligand disc on (4000-400) cm^{-1} and using [CsI] for complex on (4000-200) cm^{-1} Shimadzu spectrophotometer and FTIR spectrophotometer. UV-Visible spectra were recorded using a Shimadzu UV-VIS 1800 Spectrophotometer to confirm formation. The static stress device was used to determine the damper's efficiency by monitoring the current and voltage. The results were obtained by the corrosion lab of the Ministry of Industry and minerals – Iraq. The elements analysis of mild steel was performed by spectro max device by the state company for Inspection and rehabilitation, Ministry of Industry and Materials.

Preparation of ligand

The ligand was made according to the instructions in the literature [18]. A general procedure for chemically graft copolymerization of Succinic Anhydride onto gelatin backbones by ring opening polymerization was conducted as follows:

(0.2 gm) of Gelatin was dissolved in (10mL) of ethanol and (3 gm, 1 mmol) of succinic anhydride was dissolved in DMF. Next, (0.1gm) of APS was dissolved in (1mL) water. Then, the mixture was placed in a polymerization bottle; the bottle was flushed with nitrogen for a few minutes while

wearing a glove, and the process was terminated at 70 °C using a water bath for 1 h. The solvent was evaporated under vacuum after obtaining the result. It was cleaned three times with diethyl ether. It was vacuum-sealed and dried at 50 °C, produced 90% with a polymer ηin=0.92 dL/g. The result was the beige color product.

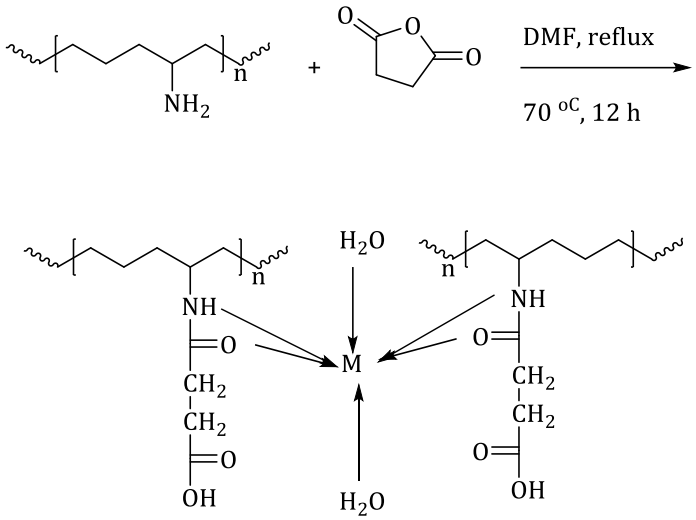

Figure 6: Synthesis of ligand

Synthesis of metal-ligand (M-L) complexes

1- Synthesis of CrL complex [Cr L (H_2O)$_2$]

To synthesize CrL complex (0.4 gm, 2 mmol) of ligand [3-[(hexan-2-yl) carbamoyl] propananoic acid], the powder was dissolved with ethanol absolute and the stirring was kept on at room temperature. It reacted with (0.266 gm, 1 mmol) of $CrCl_3.6H_2O$, and was dissolved in 10 mL ethanol absolute and refluxed with continuous stirring at 85 °C for 8 h. The resulting chromium complex (olive) was put in a watch glass, washed with diethyl ether, and dried using desiccators.

2- Synthesis of MnL, NiL, ZnL:

An amount of ($Ni(NO_3)_2.6H_2O$, $MnCl_2.4H_2O$, $ZnCl_2$) was dissolved in 10 mL ethanol and combined in a round, bottom flask with (ligand: dissolved in 15 mL ethanol) at a molar ratio of 1:2 (M:L) under heating and refluxed for 8 h. After filtering, the colorful desiccators were used to dry the precipitate after washing it with diethyl ether.

Table 1: Physical properties for ligand and its complexes

compounds	Melting point °C	color
L	165-175	OFF WHITE
CrL	135-150	OLIVE GREEN
MnL	160-175	LIGHT BROWN
NiL	155- 165	LIGHT GREEN
ZnL	140 -160	OFF WHITE

Results and discussion

Spectrum of Electronics

The electronic absorption spectrum was utilized to forecast the geometry based on the shape and quantity of observed peaks. The electronic spectrum of the ligand exhibited intense absorption at (301) nm (33.222) cm^{-1} attributed to the (n → π *) transition.

Cr-Complex

Cr(III) complex green color spectrum (CrL) showed three absorption bands at (602,410 and 341) nm (166.113, 24.390 and 29325) cm^{-1} assigned to $4A_2g$ (F) →$4T_2g$ (F), 4 A_2g; (F)→ $4T_1g$ (F) and 4 A_2g (F)→4 A_2g (P) transitions; the magnetic moment value was 3.81 BM suggesting an octahedral geometry [19].

Mn-Complex

Mn (II) complex pale brown spectrum (MnL) showed three bands at (762, 580 and 360) nm (13.123, 17.231 and 27.777) cm^{-1} attached to $6A_1g \rightarrow 4\ T_1g$, $6A_1g \rightarrow 4T_2g$ and $6A_1g \rightarrow 4A_1g$ +4Eg transition, respectively. The value of the magnetic moment was 4.82 BM proposing an octahedral geometry [20].

Ni-Complex

Spectrum of Ni (II) complex light green (NiL) showed three bands at (960, 766 and 382) nm (10.416, 13.054 and 26.178) cm-1 assigned to $3A_2g \rightarrow 3T_2g$, $3A2g \rightarrow 3T_1g$ (F) and $3A_2g \rightarrow 3T_1g$ (P) transition, respectively. The magnetic moment value was 2.89 BM proposes an octahedral geometry [21].

Zn-Complex

Because of the filled (d) orbital, zinc ion complexes with (d^{10}) electronic configuration were not predicted to display (d-d) electronic transition [22] in the visible region. This complex did not show a clear band, absorption band at (305) nm, (32.786) cm^{-1} attributed to charge transfer from metal to ligand [23]; the magnetic moment value was diamagnetic

Table 2: The UV- Vis spectra of the ligand and complexes

Comp	λ nm	ύ cm^{-1}	Assignments	μeff (B.M)	Structure
L	301	33.222	(n→π*)	-	-
Cr L	602 410 341	166.113 24.390 29.325	$^4A_2g \rightarrow {}^4T_1g_{(P)}$ $^4A_2g \rightarrow {}^4T_1g$ $^4A_2g \rightarrow {}^4T_2g$	3.81	Octahedral
MnL	762 580 762	13.123 17.231 27.777	$^6A_1g \rightarrow {}^4T_1g$ $^6A_1g \rightarrow {}^4T_2g$ $^6A_1g \rightarrow {}^4A_{1g} + {}^4Eg$	4.82	Octahedral
NiL	960 766 382	10.416 13.054 26.178	$^3A_2g \rightarrow {}^3T_2g$ $^3A_2g \rightarrow {}^3T_1g$ (F) $^3A_2g \rightarrow {}^3T_1g$ (P)	2.89	Octahedral
ZnL	305	32.786	Metal to ligand charge transfer	Diamagnetic	Octahedral

FTIR spectra of the ligand:

The absorption spectrum in the infrared region [FT-IR] solid sample of ligand was run in (KBr) pellet as characteristic bands, at characteristic band at 1726 cm-1 that was attributed to C=O stretching of succinic anhydride grafted to gelatin backbone. Graft copolymer product comprised a gelatin backbones with side chains that carried carboxylic acid and carobxamide functional groups evidenced by peaks at 1726, 1689 cm^{-1} related to the symmetric stretching in carboxicylat that is reconfirmed by another peak at 1543 cm^{-1} which is related to the symmetric stretching of the carboxylic band and another at 3439 cm^{-1} strong band ascribed to υ (-OH) stretch. The stretching vibrations of aliphatic (C - H) occurs at frequencies between 2989-2931 cm^{-1} [24].

FT-IR spectra of complex

The bands attributed to the (C=O) of amide of ligand, mentioned previously were shifted to lower wave number in all complex coordination through the nitrogen atom and oxygen of (C=O) and NH groups, so the ligand behaves as a bidentate. The presence of (M-O) and (M-N) bands in the spectra of complexes can be used to substantiate these claims. The relevant vibration bands of complexes were recorded in [CsI] disc in the region 200-4000 cm^{-1} [25]. In the FT-IR spectra, the significant distinctive peaks were found, which are assigned in Table 3. The presence of water in the spectra for all complexes has been suggested by the very broad absorption bands at 3464-3437 cm^{-1} and has been shown in the lower frequencies region, a new 808-642 cm^{-1} due to modes of coordination water and molecules. A few new bands have weak density observed at the areas about 518-588 cm^{-1} and in the region new weak bands observed at (470 -418) cm^{-1} have been appointed to the υ (M - N) [26]. In region a new weak bands are observed at 412-375 cm^{-1} appointed to the, υ (M - O).

Table 3: The FTIR spectra of the ligand and complexes

Complex	υ (- OH)	υ (C= O)	Amide υ (C= O)	υ(M - N)	υ(M–O)	υ(-H_2O)
L	3439	1726	1689	-	-	-
Cr L	3437	1699	1654	447	403	806
Mn L	3441	1699	1676	470	412	642
Ni L	3437	1697	1653	451	418	677
Zn L	3464	1697	1697	449	420	806

Corrosion

Corrosion is the erosion of a material's characteristics due to interactions with its environment, which is unavoidable for most metals (and many other materials) while it is most commonly connected with.

Types of Corrosion

Kinds of corrosion include Crevice, Corrosion, Stress Corrosion Cracking, Intergranular Corrosion, Galvanic Corrosion; Pitting Corrosion, and Uniform Corrosion.

Corrosion Prevention

To avert catastrophic losses, it is critical to take preventative measures. The bulk of the structures we use is made of metal. Examples include bridges, automobiles, machinery, and household goods such as window grills, doors, and railway lines. Corrosion can be prevented in various techniques, including electroplating, galvanization, painting and lubrication, and the use of corrosion inhibitors.

Chemical inhibitors are used in various ways to slow down corrosion processes. Exploration and production of oil and gas, petroleum refineries, chemical manufacture, and heavy manufacturing are examples of heavy manufacturing, water treatment, and product additive sectors utilizing corrosion inhibitors. Many publications have emerged to develop environmentally-friendly corrosion inhibitors, and a significant amount of research has gone into developing so-called "green" corrosion inhibitors. In addition, research into natural items such as plant extracts, essential oils, and refined chemicals has increased to create ecologically beneficial corrosion inhibitors. Polymer has been compared with microscopic particles. Organic compounds with higher viscosity, in contrast to small organic molecules with active polar centers and big heteroatoms on their surfaces, have more viscosity. They are more adaptable and stable than others. These active centers can readily be linked together. Polymers are simple to produce, more accessible, less poisonous, and ecologically beneficial than mineral components and tiny organic compounds. They do not pollute the environment [27,28].

Carbon steel working examples with dimensions of 6×6 cm are used. The metal specimens are put in the phosphating bath at a depth of 10 cm above the bottom of the solution and a depth of 10 cm below it.

In the carbon steel bath, the temperature is adjusted to 25 °C using a thermostat. Corrosion cells consist of 3 electrodes a platinum foil auxiliary and a saturated calomel reference electrode (SCE). The aggressive 0.5M hydrochloric acid with distilled water was used.

Potentiodynamic Polarization Measurements

The corrosion currents decrease due to the Co-polymer (gelatin grafting with succinic anhydride) molecules' adsorption at the cathodic site of the metal surface, increasing inhibitor concentration and shifting corrosion potentials in the cathodic direction [29]. The addition of the (Co- polymer (gelatin grafting with succinic anhydride) to the Hydrochloric acid solution improves the corrosion behavior and it forms a layer on a metal surface. Thus, the process is considered physical adsorption of active molecules [30-31]. Tables 1 and 2 show the corrosion protection (Ecorr), corresponding inhibitor efficiencies (I.E %), (bc) cathodic Tafel slope values deduced from the polarization curves, and (Icorr) corrosion current densities. Figures 1 and 2 show that when there is an increase in the concentration, there will be a decrease in the current, leading to the decrease of both the anodic and cathodic overpotential of carbon steel.

Table 4: Polarization data of carbon steel in the absence and presence of different concentrations of (Complex +Cr^{+3}) in 0.5M HCl solution at 298K

inhibitor Con. (ppm)	-Ecorr. (mV)	Icorr. ($\mu A.cm^{-2}$)	-bc (mv/Dec)	ba (mV/Dec)	W.L ($g.m^{-2}.d^{-1}$)	P.L ($mm.y^{-1}$)	Rp ($\Omega.cm^2$)
Blank	579.5	310.93	90.5	65.2	77.7	0.961	52.92
100	517.3	94.47	93.0	62.3	25.4	0.618	171.48
200	460.9	73.75	74.9	68.0	17.8	0.511	209.85
500	473.1	55.48	68.8	78.4	13.9	0.361	286.79

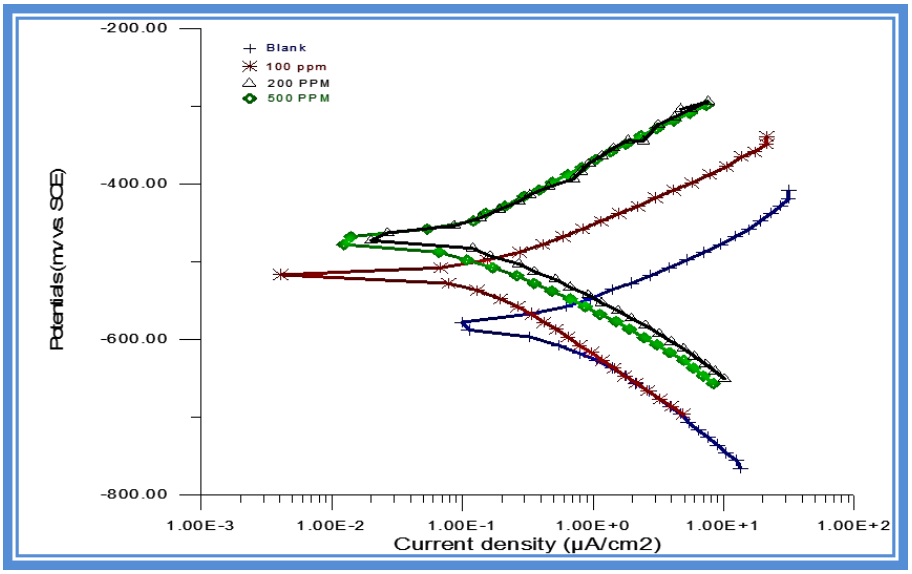

Figure 7: Potentiodynamic Polarization curve of carbon, steel with different concentrations: of (Complex + Cr^{+3}) in 0.5MN HCl at 25 °C

Table 5: Polarization data of carbon steel, in the absence and presence of different: concentrations of (Complex +Zn^{+2}) in 0.5M HCl solution at 298K

inhibitor Con. (ppm)	-Ecorr. (mV)	Icorr. ($\mu A.cm^{-2}$)	-bc (mv/Dec)	ba (mV/Dec)	W.L ($g.m^{-2}.d^{-1}$)	P.L ($mm.y^{-1}$)	Rp ($\Omega.cm^2$)
Blank	579.5	310.93	90.5	65.2	77.7	0.961	52.92
100	516.4	46.82	102.0	68.1	11.7	0.543	378.72
300	486.6	45.16	66.4	78.9	0.946	0.439	346.68
500	480.5	43.80	65.3	79.9	0.122	0.331	356.23

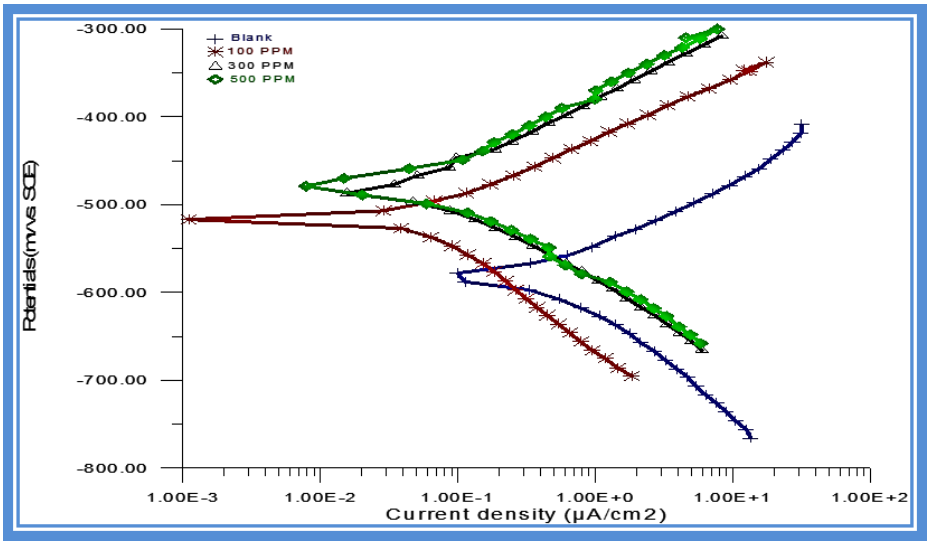

Figure 8: Potentidyna, Polarization curve of carbon steel with different concentrations of (Complex +Zn^{+2}) in 0.5M HCl: at 25 °C

Effect of (Complexes+$Cr^{+3}$and Zn^{+2}) concentration

Table 6 indicates that adding ((Complexes+Cr^{+3} and Zn^{+2})) to carbon steel in 0.5M hydrochloric acid at 298 K temperatures reduces corrosion rates. The adsorption of inhibitor and surface coverage metal increase with increasing the inhibitor concentration [31-33].

Table 6: shows the values of corrosion rates, inhibition efficiency (%IE) and (θ) surface coverage degree for carbon steel corrosion without and with the addition of different concentrations of (Complexes+Cr^{+3} and Zn^{+2}) in 0.5 M hydrochloric acid solution at 298K.

Table 6: investigation of adding ((Complexes+Cr^{+3} and Zn^{+2})) to carbon steel

Inhibitor Con. (ppm)	Temperature (K)	Corrosion Rate ($g/m^2.d$)	Surface Coverage Degree (θ)	Inhibition Efficiency % IE
Blank	298	143.61	0.00	0.00
(Complexes + Cr)				
100	298	43.63	0.6962	69.62
200		34.06	0.7628	76.28
500		25.62	0.8216	82.16
(Complexes + Zn)				
100	298	21.62	0.8495	84.94
300		20.86	0.8547	85.48
500		20.23	0.8591	85.91

Conclusion

In this work, we prepared polymer by grafted Gelatin with succinic anhydride and ring opening polymerization of succinic anhydride by Gelatin, and complexes with Cr, Mn, Ni, Zn. and studied the application of inhibiter of corrosion for complexes of Cr and Zn.

In this research study, the metal-carbon steel dissolution in 0.5M HCl solution was protected by using (Complex Cr^{+3}+Zn^{+2}), potentiodynamic polarization and weight loss (W.L). It has been shown that these corrosion inhibitors make carbon steel protection. The inhibition activity (complexes Cr^{+3}+Zn^{+2}) could block the influence by the adsorption of inhibitor molecules on the carbon steel surface

Funding

This research did not receive any specific grant from fundig agencies in the public, commercial, or not-for-profit sectors.

Authors' contributions

All authors contributed toward data analysis, drafting and revising the paper and agreed to responsible for all the aspects of this work.

Conflict of Interest

We have no conflicts of interest to disclose.

ORCID

Zahraa A.Rida

https://www.orcid.org/0000-0002-1981-8174

References

[1]. Stevens P., *Food stabilisers, thickeners and gelling agents*, Wiley-Blackwell, 2009, 116 [Google Scholar], [Publisher]

[2]. Saxelin M., Pessi T., Salminen S., *Int. J. Food Microbial.*, 1995, **25**:199 [Crossref], [Google Scholar], [Publisher]

[3]. Schrieber R., Gareis H., *Gelatine handbook: theory and industrial practice*. John Wiley & Sons; 2007 [Google Scholar], [Publisher]

[4]. Yang C.L., Sun Y.H., Yu W.H., Yin X.Z., Weng J., Feng B., *Eur. Cells Mater.,* 2018, **36**:15 [Google Scholar]

[5]. Sweedman M.C., Tizzotti M.J., Schäfer C., Gilbert R.G., *Carbohydr. Polym.,*. 2013, **92**:20. [Crossref], [Google Scholar], [Publisher]

[6]. Hui R., Qi-He C., Ming-liang F., Qiong X., Guo-qing H., *Food Chemistry.* 2009, **114**:6 [Crossref], [Google Scholar], [Publisher]

[7]. Tesser R., Vitiello R., Russo V., Turco R., Di Serio M., Lin L., Li C., *InIndustrial Oil Plant,* 2020, 201-268 [Crossref], [Google Scholar], [Publisher]

[8]. Han C.G., Qian X., Li Q., Deng B., Zhu Y., Han Z., Zhang W., Wang W., Feng S.P., Chen G., Liu W.,

Giant thermopower. Science. 2020, **368**:1091 [Crossref], [Google Scholar], [Publisher]
[9]. Baumgartner M., Hartmann F., Drack M., Preninger D., Wirthl D., Gerstmayr R., Lehner L., Mao G., Pruckner R., Demchyshyn S., Reiter L., *Nat. Mater.,* 2020, **19**:1102 [Crossref], [Google Scholar], [Publisher]
[10]. Qiao C., Ma X., Zhang J., Yao J., *Food Chem*., 2017**,** **235**:45 [Crossref], [Google Scholar], [Publisher]
[11]. Krishnamoorthy S., Noorani B., Xu C., *Int. J. Mol. Sci.*, 2019, **20**:5061 [Crossref], [Google Scholar], [Publisher]
[12]. Bello A.B., Kim D., Kim D., Park H., Lee S.H., *Tissue Eng. Part B Rev.*, 2020, **26**:164 [Crossref], [Google Scholar], [Publisher]
[13]. Zhang L., Liu J., Zheng X., Zhang A., Zhang X., Tang K., *Carbohydr. Polym.,* 2019, **216**:45 [Crossref], [Google Scholar], [Publisher]
[14]. Al-Shafey H.I., Hameed R.A., Ali F.A., Aboul-Magd A.E., Salah M., *Int. J. Pharm. Sci. Rev. Res.*, 2014, **27**:146 [Google Scholar], [Publisher]
[15]. Al-Shafey H.I., El Azabawy O.E., Ismail E.A., *J. Dispers. Sci. Technol*., 2011, **32**:995 [Crossref], [Google Scholar], [Publisher]
[16]. Kumar S.H., Karthikeyan S., Narayanan S., Srinivasan K.N., *Int. J. Chem. Tech. Res*., 2012, **4**:1077 [Google Scholar]
[17]. Yingsamphancharoen T., Rodchanarowan A., *Technology*, 2019, **10**:192 [Google Scholar], [Publisher]
[18]. Williams R.J., Da Silva J.F., *J. Theor. Biol.,* 2003, **220**:323 [Crossref], [Google Scholar], [Publisher]
[19]. Shen X., Yang X., Su C., Yang J., Zhang L., Liu B., Gao S., Gai F., Shao Z., Gao G., *J. Mater. Chem. C,* 2018, **6**:2088. [Crossref], [Google Scholar], [Publisher]
[20]. Azab A.A., Ateia E.E., Esmail S.A., *Appl. Phys. A*, 2018, **124**:469 [Crossref], [Google Scholar], [Publisher]
[21]. Yamane S., Hiyoshi Y., Tanaka S., Ikenomoto S., Numata T., Takakura K., Haraguchi T., Palafox M.A., Hara M., Sugiyama M., Akitsu T., *J. Chem.,* 2017, **11**:135. [Crossref], [Google Scholar], [Publisher]
[22]. Passos G.F., Gomes M.G., Aquino T.M., Araújo-Júnior J.X., Souza S.J., Cavalcante J.P., Santos E.C., Bassi Ê.J., Silva-Júnior E.F., *Pharmaceuticals*, 2020, **13**:141 [Crossref], [Google Scholar], [Publisher]
[23]. Guo Y., Hao Y., Gao L., Hao H., *Crystals,* 2020, **10**:92 [Crossref], [Google Scholar], [Publisher]
[24]. Rathod V., Anupama A.V., Kumar R.V., Jali V.M., Sahoo B., *Vib. Spectrosc.*, 2017, **92**:267 [Crossref], [Google Scholar], [Publisher]
[25]. Wang Y., Hu X., Guo T., Tian W., Hao J., Guo Q., *Chem. Eng. J.,* 2021, 416:129007 [Crossref], [Google Scholar], [Publisher]
[26]. Saei E., Ramezanzadeh B., Amini R., Kalajahi M.S., *Corros. Sci.,* 2017, **127**:186 [Crossref], [Google Scholar], [Publisher]
[27]. Verma C., Ebenso E.E., Bahadur I., Quraishi M.A., *J. Mol. Liq.,* 2018, **266**:577 [Crossref], [Google Scholar], [Publisher]
[28]. Hameed R.A., Al-Shafey H.I., Abu-Nawwas A.H., *Int. J. Electro. Chem. Sci.,* 2014, **9**:6006 [Google Scholar]
[29]. Al-Shafey H.I., Hameed R.A., Ali F.A., Aboul-Magd A.E., Salah M., *Int. J. Pharm. Sci. Rev. Res.,* 2014, **27**:146 [Google Scholar], [Publisher]
[30]. Fathima H., Pais M., Rao P., *J. Bio. Tribo. Corros.,* ,2021, **7**:108 [Crossref], [Google Scholar], [Publisher]
[31]. Xhanari K., Grah N., Finšgar M., Fuchs-Godec R., Maver U., *Chem. Papers,* 2017, **71**:81 [Crossref], [Google Scholar], [Publisher]
[32]. Zarei A., Mardi K., *Chem. Methodol.,* 2021, **5**:513 [Crossref], [Google Scholar], [Publisher]
[33]. Al-mashhadani M.H., Ahmed A.A., Hussain Z., Mohammed S.A., Yusop R.M., Yousif E., *Al-Qadisiyah J. Pure Sci.,* 2020, **25**:1 [Crossref], [Google Scholar], [Publisher]

HOW TO CITE THIS ARTICLE
Zahraa A. Rida, Sahar S. Hassan, Sana H.Awad. Synthesis and Characterization of New inorganic Complexes and Evaluation Their Corrosion Inhibiter. *Chem. Methodol.*, 2022, 6(4) 347-356
https://doi.org/10.22034/CHEMM.2022.326331.1431
URL: http://www.chemmethod.com/article_146760.html